



Review article

3D Printing of parts using metal extrusion: an overview of shaping debinding and sintering technology

*Luigi Maria Galantucci, Alessandro Pellegrini, Maria Grazia Guerra, Fulvio Lavecchia

Politecnico di Bari, Dipartimento di Meccanica Matematica e Management Via Edoardo Orabona, 4 - 70125 Bari – Italy

ABSTRACT

Additive Manufacturing (AM) is the fabrication of real three-dimensional objects from plastics and metals by adding material, layer by layer. One of the most common AM processes is the Material Extrusion (ME) based on different approaches: plunger, filament and screw. Material Extrusion technologies of metal-polymer composites is expanding and it mainly uses the filament or plunger-based approaches. The feedstock used is a mixture of metal powder (from 55 vol% to about 80 vol%) dispersed in a thermoplastic matrix, as the Metal Injection Molding (MIM) materials. The process consists of three steps: shaping, debinding and sintering. The first step provides the extrusion of filament to realize a primary piece called "green part"; subsequent steps, debinding and sintering, allow to obtain a full metal part by dissolving the polymeric binder. The latter can be carried out using solvents, heat and the combination of them. The interest toward this technology is driven by the possibility to replace other Metal AM technologies, such as Selective Laser Melting or Direct Energy Deposition, in sectors like rapid-tooling or mass production, with several benefits: simplicity, safety to use and saving material and energy. The aim of this keynote is to provide a general overview of the main metal ME technologies considering the more technical aspects such as process methodologies, 3D printing strategy, process parameters, materials and possible applications for the manufacturing of samples on a 3D consumer printer.

Key words: Fused Filament Fabrication, Metal Extrusion, SDS process;

1. INTRODUCTION

Several Additive Manufacturing processes are currently existing; they only differ in the way layers are deposited to create an object, in the operation modes and in the way the material is fed into the system. Some methods melt or soften materials (thermoplastics, composites, photopolymers and metals) to produce the layers, e.g., Material Extrusion (ME) or Fused Filament Fabrication (FFF), Selective Laser Sintering (SLS), Selective Laser Melting (SLM) and Electron Beam Melting (EBM), Direct Metal Laser Sintering (DMLS), while others cure liquid materials, e.g., Stereolithography (SLA) [1]. However, it is necessary for SLS, SLM and DMLS techniques to adopt high-energy beams including laser or electron beam as heating sources to fuse the metal powders during the whole manufacturing processing to obtain metal parts, which is very energy-consuming. In addition, these techniques usually require large investments for metal powders, machinery, and maintenance, limiting their applications

mainly to the high value-added industries which are cost-insensitive. Therefore, it is of practical significance to explore other economical metal 3D printing techniques with less energy consumption. Material Extrusion, conversely, is a cheaper 3D printing technique mainly developed for the additive manufacturing of polymer materials. During the manufacturing process, a polymeric filament is first melted in the printing nozzle at a temperature slightly higher than the melting point of the printing polymer, then deposited onto the printer hot bed layer by layer under the control of a computer, and finally fused with the bottom adjacent layers [2]. Whenever necessary, support structures are included in the process to enable the fabrication of complex geometrical features. This basic principle enables the production of complex parts without a shaping tool other than a die with a simple geometry. Depending on the type of extruder used, one can classify material extrusion into different types: filament and plunger-based [3]. The first example of using FFF for the production of metal parts was presented in 1996 with a

*Corresponding author's e-mail: luigimaria.galantucci@poliba.it

Published by the University of Novi Sad, Faculty of Technical Sciences, Novi Sad, Serbia.
This is an open access article distributed under the CC BY-NC-ND 4.0 terms and conditions

17-4 PH stainless steel and tungsten carbide-cobalt [4,5] and this process was later on referred as FDMet (Fused Deposition of Metal) or Metal Fused Filament Fabrication (Metal FFF) [6]. This new AM method is based on the combination of FFF and Metal Injection Molding (MIM), a more conventional process which allows to obtain a close full density metal part with high complexity. The feedstock used is a mixture of metal powders with a different amount in percentage by volume (vol%) from 55 since to 88, as reported in open library, and a polymeric binder. This is constituted by three different component: a main binder (i.e., Polyoxymethylene (POM), Wax paraffin, Thermoplastic elastomer (TPE) or Polyethylene glycol (PEG)), a backbone binder like Polypropylene (PP), Low-Density Polyethylene (LDPE) or Grafted Polyolefin and in some cases also additives like stearic acid, the most common [3,7–9]. The printed part is defined as “Green Part”, the debinded part as “Brown Part”, and the sintered metal part as “White Part”, respectively, while the entire process chain is called “Shaping, Debinding and Sintering-SDS-Process”. In the first step, the green parts are printed from metal/polymer composite filament, during which polymer is melted as the binder but the metal particles remain solid subsequently, brown parts were obtained by subjecting the green parts to a debinding process to remove most of the polymer binder. The remaining polymer binder in the brown parts avoid the spreading of the metal particles and thus preserve the shape of the parts. Finally, they are sintered to melt the metal particles together to form a dense material.

2. TYPES OF METAL EXTRUSION

2.1 Tensile Strength

The first way to extrude the filament and realize the green parts is the “filament-based” type (Fig.1).

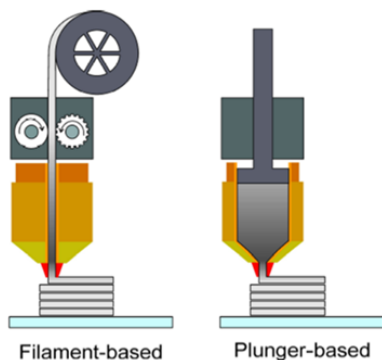


Fig.1 Type of Material Extrusion [3]

The American company Markforged Inc. has realised a hybrid-process inspired by Metal FFF named Atomic Diffusion Additive Manufacturing TM (ADAM). The entire SDS process of Markforged system is controlled by a proprietary software called “Eiger”. The printing of green part takes place in the “Metal X” printer equipped with a heated nozzle of 0.4 mm, which softens and deposits material layer by layer with a height equal to 125 µm. As

reported in Eiger slicer, this is the unique layer height available. Only for copper, the layer height is 129 µm. The feedstock used is a spool of different materials like: stainless steel 17-4 PH or H13, A2 and D2 tool steel, but also nickel superalloy (Inconel 625) and copper [10]. The used binder is completely thermally debound in the washing system with proprietary solvent (Opteon SF79, Opteon SF80, or Tergo Metal Cleaning Fluid). The last step useful for the realization of a dense metal part is the sintering, which varies in terms of temperatures and the time according of the selected material. Some examples of parts printed via ADAM are reported in Fig.2.



Fig. 2 Examples of parts made via ADAM in 17-4 PH [11]

On the other hand, the German society BASF 3D Printing Solutions GmbH, offer two metal-composite filaments called Ultrafuse® 316L and Ultrafuse® 17-4 PH, opening the possibility to produce green parts with existing and, in some cases, very cost-effective, FFF printers, as shown in Fig. 1.

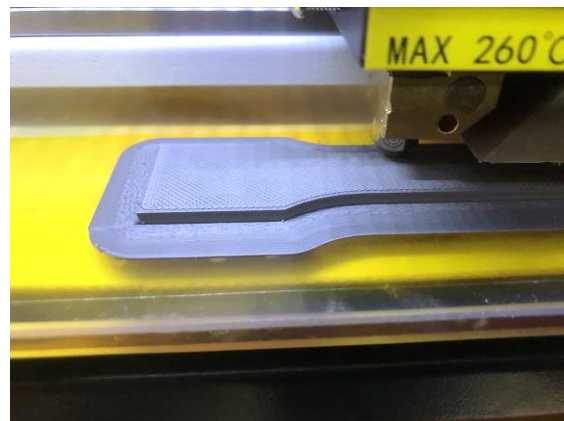


Fig. 1 Example of printing of sample in Ultrafuse 316L with a consumer 3D printer

Then, also in this case, the green parts are processed into pure metal parts using a debinding and sintering process [12].

The metal/polymer composites filament consists of a polymer matrix and an 88 vol% dispersed stainless steel particles with a different particle size. In Ultrafuse 316L filament, variable particle size of metal powder are

dispersed in the matrix; they are indicated with white arrows in Fig. 2. Typical dimensions of metal powder grains are comprised in the range 1-10 μm , according to Tosto et al. [13], while Liu et al. [2] observed higher values, comprised between 30-50 μm . The polymer matrix (red arrows in Fig. 2), is composed of POM and Polyethylene (PE) with other additives such as polypropylene, dioctyl phthalate (DOP), dibutyl phthalate (DBP), and zinc oxide (ZnO) to increase the fluidity, plasticity, and thermo-stability of the composite [2].

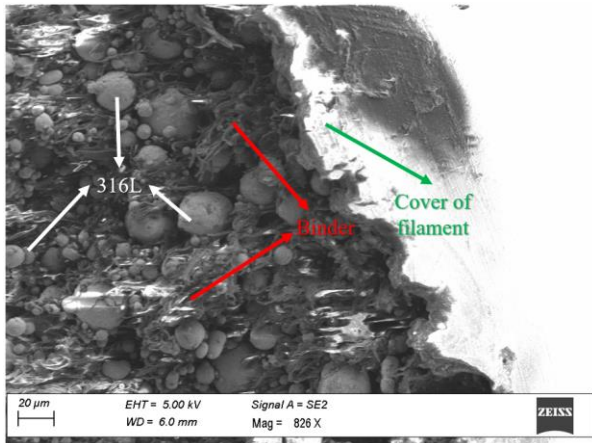


Fig. 2 SEM image of cross section of Ultrafuse 316L filament

In research laboratories, in other cases, it is possible to manufacture filaments with different percentage of metal and polymer [6,14–22]. In particular, it is possible to use stainless-steels, (316L and 17-4 PH the most common ones), titanium alloys (Ti-6Al-4V) [14,20], hard-metals like carbide tungsten (WC) and tungsten carbide-cobalt (WC-Co) [18] and low-melting alloys (low-melting eutectic alloy of bismuth, non-eutectic alloy of bismuth, and a non-eutectic alloy of antimony) [21]. For the manufacturing of filament, it is necessary that it keeps a constant and uniform diameter during the entire process in order to maintain a constant delivery rate for a good printing result. The filament is usually manufactured using a single or twin-screw extruder. In addition, the material to be processed should have an even distribution of the binder, which should be easy to remove from the metal powder (by debinding or burning/evaporation). It is required a good fineness of metal powder to manufacture metal filaments. A uniform, as small as possible, size of the metal particles is important in order to obtain a uniform filament, to produce uniform prints and reproducible sintering results. It is a good practice to use grain sizes in the range between 2 and 44 μm . According to Thompson et al. [6] the average size of metal powder for a 316L is 17.7 μm . The metal is preliminarily treated with an agent able to reduce the interaction forces between the particles and to lubricate the powder. Cyclohexane or stearic acid are the most used for this treatment. The metal powder is then gradually mixed with the polymer binder. The amount of metal powder is relevant for achieving a lower residual porosity after debinding and a better densification due to higher number of particle contacts.

Consequently, a high content of metal powder can generate voids and inhomogeneity in the extruded profiles due to higher feedstock viscosity and increasing particle friction [23]. The uniformity of distribution of the material components can be estimated through the viscosity of the mixed material and, therefore, through the torque value of the mixing device driving motor. Usually, due to the high metal content of these materials, it is recommended a nozzle in hard metal or ruby, with a diameter ≥ 0.4 mm [24].

2.2. Plunger based process

The second extrusion type is the “plunger-based” (Fig.1). Another American company, Desktop Metal Inc. has patented a technology similar to FFF and MIM process called Bound Metal Deposition™ (BMD) enabling the printing of bound metal rods and the subsequent sintering to form a dense metal part. In the BMD process, the desired metal or alloy powder is compounded with an appropriate multi-component organic binder system to form the feedstock. The feedstock is shaped into a rod that has a well-defined and controlled diameter. Multiple rods of a fixed diameter and length are housed in a specially designed and padded dispensing cartridge. The cartridge feeds rod to an extruder which actuates and heats the rods to produce a quasi-molten composite. This composite is easily pushed by a plunger through a 0.4 mm nozzle, while the extruder moves on the build plate following a predetermined path to produce the green parts (Fig. 3). This extrusion system enables precise printing and a minimum layer height of 50 μm . In cases where the three-dimensional complexity of a part requires support structures to be printed, an interface layer is included in the design to allow for later separation [18,25].



Fig. 3 Example of green parts printed via BMD in 17-4 PH stainless steel

Desktop Metal’s materials available are similar to the ones provided by Markforged: 17-4 PH stainless steel, H13 tool steel and copper, but also 316L stainless steel and 4140 low alloy steel [26]. The binder used by Desktop Metal system is first debound by a solvent and then treated thermally. Later, there a sintering process is necessary to obtain a metal part. As Markforged, Desktop Metal provides a proprietary system composed by the 3D printer, debinder

and furnace for sintering governed by a proprietary software called “Fabricate”.

3. SDS PROCESS

3.1 Shaping

The first phase of process is the shaping. In this phase the filament is extruded layer by layer until the entire green part is obtained. A right combination of printing parameters, such as infill density, flow rate, layer height and printing speed influence the success of print. In fact, when this does not happen, some troubles could be detected, such as a not perfect adhesion of the roads, which causes an incorrect filling of the green part, and subsequent voids in the metal part. In Fig. 4 three objects printed are shown; varying the flow rate, evident voids are created on the surface of these objects.

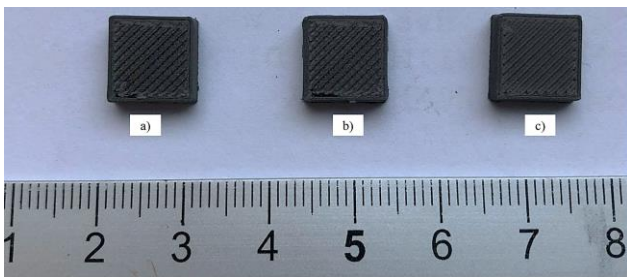


Fig. 4 Example of green parts with non-perfect adhesion between the rods

Keeping constant the infill at 100% and the printing speed at 35 mm/s, instead increasing the flow rate from 110% (a) to 115% (b) and 125% (c), it has been possible to avoid the voids present in the first two parts. This behavior is confirmed from microscope images (Fig. 7) of these objects: in the a) and b) part holes in the vicinity of the wall layers also appear.

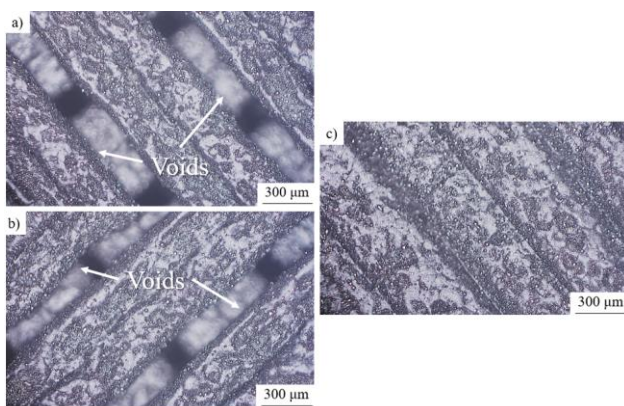


Fig. 5 Image at optical microscope of the green parts (140x)

3.2. Debinding

Once the green part is printed, the polymeric binder must be removed. This process is commonly referred to as “debinding” and it is very well known for parts produced

by MIM. Polymers have to be removed completely from the green part since carbon residues can influence the sintering process and negatively affect the quality of the final product. Moreover, binder removal is one of the most critical steps in the SDS process, since defects can be produced by inadequate debinding. Some examples are blistering, surface cracking, and large internal voids. There are three main debinding techniques: thermal, solvent, and catalytic methods [3]. For a solvent debinding, the treatment time varies depending on the shape and size of the printed parts. Gonzalez-Gutierrez et al. [27] suggest that printed parts should be kept in the solvent for at least 12 h. The same procedure is suggested by Thompson et al. [6] for parts having a wall thickness of 2 mm, while for a wall thickness of 6 mm the removing processing time of TPE should be 57 h. Removal of TPE of the printed green bodies generates interconnected pore channels. During solvent debinding, elimination of at least 99% of the contained TPE mass is necessary in order to enable successful realization of the following process steps. As rule, the mass loss of printed parts should be monitored during the debinding to determine the end of the treatment. Thermal debinding is performed by heating the parts in a vacuum furnace with a variation of pressures between 10^{-3} to 10^{-5} mbar, depending on variable levels of volatilized binder within the furnace during the burnout process. Debinding temperatures has to be evaluated in accordance with thermogravimetric analysis (TGA) of the backbone polymer. Heating rates have to be as high as possible, but slow enough to avoid blistering or crack formation within the samples [6]. Some studies proposed different temperatures depending on the geometry of the part and the material; Thompson et al. [6] observed the complete degradation of backbone binder at 500 °C on a 316L stainless steel filament. Supriadi et al. [28] found the optimum debinding temperature for a 17-4 PH stainless at 510 °C, with a binder removal percentage of 6.2% and fewer oxides content. Choi et al. [29] studied the sintering of 316L stainless steel, and found that the weight loss of the molded part started at about 180 °C, and the weight became constant around 400 °C, with a percentage of 5.70%. Thermal debinding can take place even after a solvent debinding, in the same furnace of sintering; in fact it is considered a preliminary sintering [30]. The last type of debinding is the catalytic debinding. This process is patented by BASF SE [31] for their metal-composite filament, but also for MIM feedstock, such as Catamold®. In fact, Catamold is totally unique in its ability for the catalytic gas phase decomposition of the binder and this ability is innate to the chemical structure of POM (Fig. 6). The oxygen atoms in the polymer chain are susceptible to acidic attack, causing the macro-molecule to split off successively CH_2O (formaldehyde) units when it is exposed to a suitable acidic catalyst and nitrogen dioxide (NO_2). The catalyst used for the debinding process is gaseous nitric acid (HNO_3), with a concentration higher than 98,5% [32]. First the exhaust is burned in a reducing atmosphere (no oxygen and rich in nitrogen) at a temperature of 600 °C, transforming nitric dioxide into nitrogen gas (N_2). The second step consists is the burning

in an oxidizing atmosphere at 800 °C to transform formaldehyde into water and carbon dioxide. It is important to mention that binders based on POM usually have a backbone polymer which is not susceptible to catalytic debinding. Such backbone polymer helps retain strength and shape stability in the “brown part”. However, sintering cannot begin until this backbone polymer is still present, and thus a thermal treatment between 200 and 600 °C is applied to the part prior to the start of the sintering process [8]. The guidelines of BASF for the catalytic debinding of green parts realized by FFF and MIM recommend a temperature between 110-120 °C, with a debinding rate of 1-2 mm/h and a holding time variable depending on the material weight in the furnace. The debinding process terminate when a minimal debinding loss of 10.5% is reached.

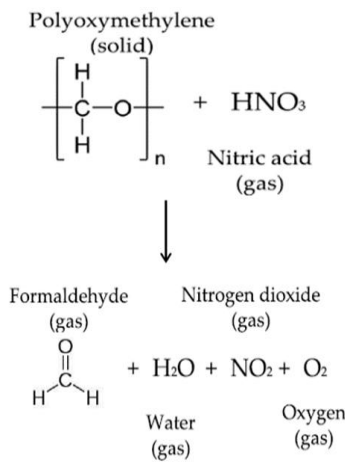


Fig. 6 Mechanism of decomposition of POM [8]

3.3. Sintering

The sintering is the last step necessary to obtain a full dense metal part realised via FFF or MIM. In general, this process is performed at temperatures below the melting temperature of the major constituent in the metal, typically ranging from 1200 to 1600 °C. Also, the holding time is related to material and size of part. For small parts such as bushings, the average time varies from 1 to 1.5 h; for average-size ferrous parts, the sintering time can be 3 h. However, tungsten parts can have a sintering time of up to 8 h [8]. An important aspect to consider during sintering is the atmosphere inside the furnace. For low carbon iron/nickel steels and stainless steels, pure hydrogen is used. To obtain low-alloy steels containing carbon, this latter is introduced via the metal powder. During sintering under nitrogen, the carbon diffuses in the metal. It is not feasible to introduce or partially remove carbon via the sintering atmosphere, since this encounters considerable difficulties in practice. Stainless steels can also be sintered under reduced pressure. With appropriate process control, even the extremely low carbon content of stainless steels can be attained. BASF AG reports different examples of sintering atmosphere used for MIM process. For example, hydrogen is recommended for a 316L for a 430 stainless

steels, but it is also possible use vacuum atmosphere. On the other hand, for a 17-4 PH stainless only hydrogen in atmosphere is recommended.

Sintering is essentially to remove pores; this is accompanied by growth and strong adhesion among the adjacent particles (Fig. 7), causing the shrinkage of the product whose dimensions usually reduce between 14 and 20%.

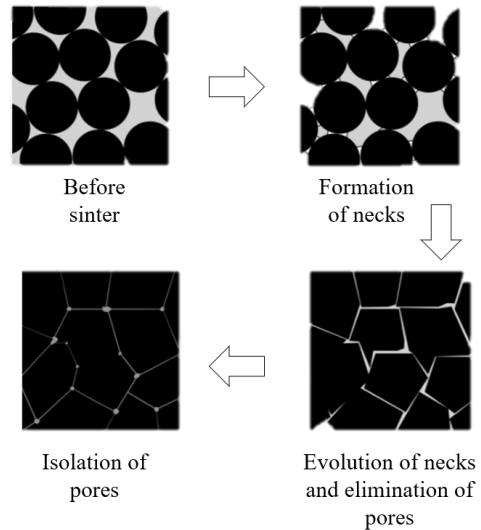


Fig. 7 Creation of pores after sintering process

The different choice of sintering parameters (holding time, temperature and atmosphere) caused different responses in mechanical aspects, as reported in Fig. 8. The graph reported shows the values recorded of mechanical properties like the Ultimate Tensile Strength (UTS), Yield Strength (YS) and the Elongation at break (ϵ_b %) for a same material (17-4 PH stainless steel) provided by different companies.

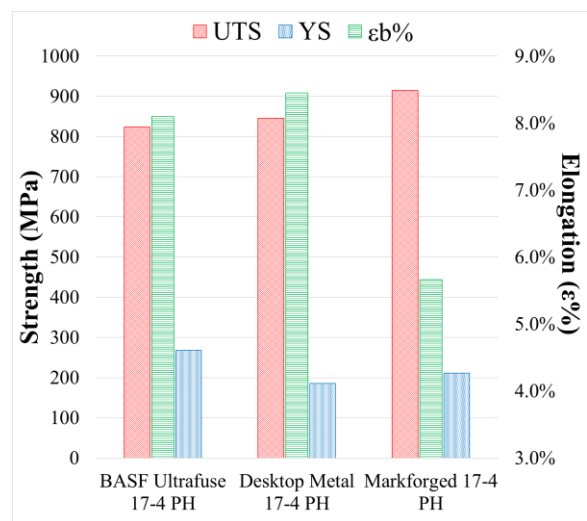


Fig. 8 Comparison of main mechanical properties for three different 17-4 PH stainless steel

3.3.1. Shrinkage Phenomenon

The green parts before printing, are oversized to compensate for the sintering shrinkage. [8] It is important to remark that the shrinkage does not occur in the same amount in all dimensions, as observed by Thompson et al. [6] and Kurose et al. [22] in samples printed with filament filled with respectively 55 vol% and 60 vol% of 316L stainless steel. Gong et al. [33,34] and Quarto et al. [35] have reported a similar shrinkage on X-Y axes, while a different one on Z axis, on a BASF Ultrafuse 316L, as found in parts printed by BMD in 17-4 PH and W-Cr [18,36]. On the contrary, Liu et al. [2] observed an equal shrinkage of 17% on all axes in 316L parts. With regard to the above, BASF 3D Printing Solutions GmbH in its guidelines, gave a nominal shrinkage for parts made in Ultrafuse® 316L and 17-4 PH: 16% on X-Y directions and 20% on Z direction [31]. The anisotropic shrinkage it was also found in parts manufactured by MIM [37]. Causes of this different shrinkage for a MIM process are to be pointed at polymer orientation which can be influenced by injection molding parameters. Besides polymer orientation, in filament highly filled, shrinkage and density can be influenced by the presence of gaps among deposited strands. The more gaps, the larger the shrinkage and the lower the density of the sintered parts, since larger gaps cannot be closed during sintering. The shrinkage can also be affected by the orientation of the filler particles [3]. Once sintering process is finished, the samples are subjected to cooling in the same furnace. Cooling is done in a protective atmosphere, in order to prevent oxidation of sintered parts.

3.4. Mechanical properties

The mechanical aspect is one of the most important, when a metal part is realized in AM. Parts printed in Metal FFF

typically report worst mechanical properties if compared to the other Metal AM technology. The main cause is the not complete fullness of the parts, caused by some problems during the SDS process and the limitation of the ME technology. In Table1 is reported a summary of some previous activities using stainless steel with compare to the data sheet and SLM technology.

3.5. Possible applications

The production of components in Metal ME is currently concentrated on few sectors: the most popular application for these technologies are Rapid tooling and prototyping. Thanks to the post-treatment capacity of sintered parts through machine tools, it could be possible to extent in the future the applications to other sectors, such as consumer goods or repair. Actually, limitations still exist for this technology related to the mechanical properties of these parts. Expansion of this technology also in others sectors required an increment of the precision and speed of printing, and an additional reduction of manufacturing cost.

4. CONCLUSIONS

Metal Extrusion is a new area of the most common AM process, Fused Filament Fabrication. For a full dense metal part, accurate dosing of metal powder and polymeric binder is necessary to avoid problems like porosity, low density or voids. In order to obtain a full metal part, the SDS process must be performed. Shaping requires an adequate choice of printing parameters.

Debinding can be execute with different methods to eliminate part of polymeric matrix, then during sintering the rest of polymer is burned and the grains of metal powder binded together. From a dimensional point of view,

Table 1 Summary table of mechanical properties

Material	Technology	Tensile strength (MPa)	Yield strength (MPa)	Tensile modulus (GPa)	Elongation at break (%)	References
17-4 PH	BMD	776	604	176	6.7	[36]
	BMD	1042	660	195	8.5	[37]
	ADAM	1050	800	140	5	[38]
	FFF	880	680	-	5.8	[39]
	FFF	497.40±9.90	443±6.90	108±6.90	0.79±0.05	[12]
	SLM	944	570	-	50	[40]
316L	FFF	465	167	152	31	[32]
	SLM	648	541	320	30	[32]
	FFF	436	167	152	-	[33]
	FFF	443.90± 5.87	148.01± 4.50	157.24± 4.50	43.33± 2.53	[12]

it is fundamental to take into account the phenomenon of shrinkage occurring during D&S, so the design of the part needs an oversizing factor for each of the three axes. Mechanical characteristics are lower if compared to parts made by SLM, however could satisfy the required strength requirements. Possibility to print metal on a traditional FFF printer or purchase an entire ME system, has allowed to expanding the material portfolio of this technology and it has changed manufacturing scenarios in different sectors. Metal Extrusion could be an economical alternative to Powder Bed technologies for the type of material used, the safety in handling it. In fact, there are not specific recommendations when printing metal filaments, lower energy cost are needed compared to laser-beam or electron-beam technologies, and the ease of use of the machine can expand the application scenario of ME.

ACKNOWLEDGEMENT

Authors want to thank CMF Marelli s.r.l., Crea 3D s.r.l and Energy Group s.r.l. for their contribution to the production of samples.

FUNDING

This research received funding from the project PON “R&I” 2014- 2020 ARS01_00806 “Soluzioni Innovative per la qualità e la sostenibilità dei processi di ADDitive manufacturing”.

This work was supported by the Italian Ministry of Education, University and Research under the Programme “Department of Excellence” Legge 232/2016 (Grant No. CUP - D94I18000260001).

REFERENCES

- [1] Ojogba, Spencer, O.: Additive Manufacturing Technology Development, A Trajectory Towards Industrial Revolution, *Am. J. Mech. Ind. Eng.* 3 (2018) 80. doi:10.11648/j.ajmie.20180305.12.
- [2] Liu B., Wang Y., Lin Z., Zhang T.: Creating metal parts by Fused Deposition Modeling and Sintering, *Mater. Lett.* 263 (2020) 127252. doi:10.1016/j.matlet.2019.127252.
- [3] Gonzalez-Gutierrez J., Cano S., Schuschnigg S., Kukla C., Sapkota J., Holzer C.: Additive manufacturing of metallic and ceramic components by the material extrusion of highly-filled polymers, A review and future perspectives, *Materials (Basel)*. 11 (2018). doi:10.3390/ma11050840.
- [4] Agarwala M.K., Van Weeren R., Bandyopadhyay A., Safari A., Danforth S.C., Priedeman W.R.: Filament Feed Materials for Fused Deposition Processing of Ceramics and Metals, *Proc. Of the Solid Free. Fabr. Symp.* (1996) 451–458. <http://hdl.handle.net/2152/70277>.
- [5] Wu G., Langrana N.A., Rangarajan S., Mccuiston R., Sadanji R., Danforth S., Safari A.: Fabrication of Metal Components using FDM, *Fused Deposition of Metals, Proc. Solid Free. Fabr. Symp.* (1999) 775–782.
- [6] Thompson Y., Gonzalez-Gutierrez J., Kukla C., Felfer P.: Fused filament fabrication, debinding and sintering as a low cost additive manufacturing method of 316L stainless steel: *Addit. Manuf.* 30 (2019) 100861. doi:10.1016/j.addma.2019.100861.
- [7] Luquan Ren J.X. and X.L., Zhou X., Song Z., Zhao C., Liu Q.: Process Parameter Optimization of Extrusion-Based, (2017). doi:10.3390/ma10030305
- [8] González-Gutiérrez J., Stringari G.B., Emri I.: Powder Injection Molding of Metal and Ceramic Parts, Some Critical Issues for Injection Molding, *Some Crit. Issues Inject. Molding.* (2012) 65–88. <http://www.intechopen.com/books/some-critical-issues-for-injection-molding/powder-injection-molding-of-metal-and-ceramic-parts->.
- [9] Nurhudan A.I., Supriadi S., Whulanza Y., Saragih A.S.: Additive manufacturing of metallic based on extrusion process, A review, *J. Manuf. Process.* 66 (2021) 228–237. doi:10.1016/j.jmapro.2021.04.018.
- [10] Markforged Inc., 3D Printing Materials-Markforged: (2021). <https://markforged.com/materials>.
- [11] Enrique P.D., DiGiovanni C., Mao N., Liang R., Peterkin S., Zhou N.Y.: Resistance is not futile: The use of projections for resistance joining of metal additively and conventionally manufactured parts, *J. Manuf. Process.* 66 (2021) 424–434. doi:10.1016/j.jmapro.2021.04.035.
- [12] Schumacher C., Moritzer E.: Stainless Steel Parts Produced by Fused Deposition Modeling and a Sintering Process Compared to Components Manufactured in Selective Laser Melting, *2000275* (2021) 4–7. doi:10.1002/masy.202000275.
- [13] Tosto C., Tirillò J., Sarasini F., Cicala G.: Hybrid Metal/Polymer Filaments for Fused Filament Fabrication (FFF) to Print Metal Parts, *Appl. Sci.* 11 (2021) 1444. doi:10.3390/app11041444.
- [14] Zhang Y., Bai S., Riede M., Garratt E., Roch A.: A comprehensive study on fused filament fabrication of Ti-6Al-4V structures, *Addit. Manuf.* 34 (2020) 101256. doi:10.1016/j.addma.2020.101256.
- [15] Wu G., Langrana N.A., Sadanji R., Danforth S.: Solid freeform fabrication of metal components using fused deposition of metals, *Mater. Des.* 23 (2002) 97–105. doi:10.1016/s0261-3069(01)00079-6.
- [16] Wang Y., Zhang L., Li X., Yan Z.: On hot isostatic pressing sintering of fused filament fabricated 316L stainless steel – Evaluation of microstructure, porosity, and tensile properties, *Mater. Lett.* 296 (2021) 129854. doi:10.1016/j.matlet.2021.129854.
- [17] Gonzalez-Gutierrez J., Kukla C., Schuschnigg S., Duretek I., Holzer C.: Fused Filament Fabrication for Metallic Parts, (2016).

- [18] Bose A., Schuh C.A., Tobia J.C., Tuncer N., Mykulowycz N.M., Preston A., Barbati A.C., Kernan B., Gibson M.A., Krause D., Brzezinski T., Schroers J., Fulop R., Myerberg J.S., Sowerbutts M., Chiang Y.M., John Hart A., Sachs E.M., Lomeli E.E., Lund A.C.: Traditional and additive manufacturing of a new Tungsten heavy alloy alternative, *Int. J. Refract. Met. Hard Mater.* 73 (2018) 22–28. doi:10.1016/j.ijrmhm.2018.01.019.
- [19] Lengauer W., Duretek I., Fürst M., Schwarz V., Gonzalez-Gutierrez J., Schuschnigg S., Kukla C., Kitzmantel M., Neubauer E., Lieberwirth C., Morrison V.: Fabrication and properties of extrusion-based 3D-printed hardmetal and cermet components, *Int. J. Refract. Met. Hard Mater.* 82 (2019) 141–149. doi:10.1016/j.ijrmhm.2019.04.011.
- [20] Singh P., Balla V.K., Tofangchi A., Atre S. V., Kate K.H.: Printability studies of Ti-6Al-4V by metal fused filament fabrication (MF3), *Int. J. Refract. Met. Hard Mater.* 91 (2020) 105249. doi:10.1016/j.ijrmhm.2020.105249.
- [21] Warriar N., Kate K.H.: Fused filament fabrication 3D printing with low-melt alloys, *Prog. Addit. Manuf.* 3 (2018) 51–63. doi:10.1007/s40964-018-0050-6.
- [22] Kurose T., Abe Y., Santos M.V.A., Kanaya Y., Ishigami A., Tanaka S., Ito H.: Influence of the layer directions on the properties of 316L stainless steel parts fabricated through fused deposition of metals, *Materials (Basel)* 13 (2020). doi:10.3390/ma13112493.
- [23] Gonzalez-Gutierrez J., Thompson Y., Handl D., Cano S., Schuschnigg S., Felfer P., Kukla C., Holzer C., Burkhardt C.: Powder content in powder extrusion moulding of tool steel: Dimensional stability, shrinkage and hardness, *Mater. Lett.* 283 (2021) 128909. doi:10.1016/j.matlet.2020.128909.
- [24] Poszvek G., Wiedermann C., Markl E., Bauer J.M., Seemann R., Durakbasa N.M., Lackner M.: Fused Filament Fabrication of Ceramic Components for Home Use, *Lect. Notes Mech. Eng.* (2021) 121–139. doi:10.1007/978-3-030-62784-3_11.
- [25] Desktop Metal, *BMD Design Guide*, (2019) 1–15. <https://www.desktopmetal.com/> (accessed July 30, 2021).
- [26] Desktop Metal Inc., *Desktop Metal materials - engineered to perform | Desktop Metal*, (2020). <https://www.desktopmetal.com/materials>.
- [27] Gonzalez-Gutierrez J., Godec D., Kukla C., Schlauf T., Burkhardt C., Holzer C.: Shaping, Debinding and Sintering of Steel Components Via Fused Filament Fabrication, *16th Int. Sci. Conf. Prod. Eng. - CIM2017*. (2017) 99–104.
- [28] Supriadi S., Suharno B., Hidayatullah R., Maulana G., Baek E.: Thermal Debinding Process of SS 17-4 PH in Metal Injection Molding Process with Variation of Heating Rates, Temperatures, and Holding Times, 266 (2017) 238–244. doi:10.4028/www.scientific.net/SSP.266.238.
- [29] Choi J., Lee G., Song J., Lee W., Lee J.: Sintering behavior of 316L stainless steel micro – nanopowder compact fabricated by powder injection molding, *Powder Technol.* 279 (2015) 196–202. doi:10.1016/j.powtec.2015.04.014.
- [30] Afian M., Subuki I.: Sintering Characteristics of Injection Moulded 316L Component Using Palm-Based Biopolymer Binder, *Sinter. - Methods Prod.* (2012). doi:10.5772/32737.
- [31] BASF 3D Printing Solutions, *Ultrafuse 316L: User guidelines for 3D printing metal parts, BASF 3D Print. Solut. process in* (2019) 1. https://www.basf.com/global/en/who-we-are/organization/locations/europe/german-companies/basf-3d-printing-solutions-gmbh/metal-solutions/Ultrafuse_316L.html.
- [32] BASF Aktiengesellschaft, *Catamold Feedstock for Metal Injection Molding: Processing - Properties - Applications*, (2003).
- [33] Gong H., Snelling D., Kardel K., Carrano A.: Comparison of Stainless Steel 316L Parts Made by FDM- and SLM-Based Additive Manufacturing Processes, *Miner. Met. Mater. Soc.* 71 (2019) 880–885. doi:10.1007/s11837-018-3207-3.
- [34] Gong H., Crater C., Ordonez A., Ward C., Waller M., Ginn C.: Material Properties and Shrinkage of 3D Printing Parts using Ultrafuse Stainless Steel 316LX Filament, *MATEC Web Conf.* 249 (2018) 1–5. doi:10.1051/mateconf/201824901001.
- [35] Quarto M., Carminati M., D’Urso G.: Density and shrinkage evaluation of AISI 316L parts printed via FDM process, *Mater. Manuf. Process.* 00 (2021) 1–9. doi:10.1080/10426914.2021.1905830.
- [36] Watson A., Belding J., Ellis B. D.: Characterization of 17-4 PH Processed via Bound Metal Deposition (BMD), *Miner. Met. Mater. Ser.* (2020) 205–216. doi:10.1007/978-3-030-36296-6_19.
- [37] Huang M.S., Hsu H.C.: Influence of injection moulding and sintering parameters on properties of 316L MIM compact, *Powder Metall.* 54 (2011) 299–307. doi:10.1179/003258909X12502679013819.

NOTE

This paper is based on the paper presented at 14th International scientific conference MMA 2021 - FLEXIBLE TECHNOLOGIES Novi Sad, Serbia, September 23-25, 2021.